Permanent File - SSEC Publications Office

CALIBRATION OF ATS-3 IMAGES FOR QUANTITATIVE PRECIPITATION ESTIMATION

David W. Martin

Dhirendra N. Sikdar

Space Science and Engineering Center
The University of Wisconsin
Madison

July 1973

Report on NOAA Contract 03-3-022-18

Table of Contents

ACKNOWLEDGEMENTS

John T. Young and John Stout contributed substantially through several stages of this program. Richard Maconi and Michael Goldman assisted in the tedious task of data analysis. Figures were very capably drafted by Dana Wooldridge; Mrs. Helen Loeb typed most of the text.

I. Introduction

Quite early in the planning of the GARP Atlantic Tropical Experiment, it became apparent that gages, radars, and other resources for measurement of precipitation were simply inadequate; that meeting the rainfall needs of GATE would require observations on a spacial scale which could only be provided by satellites. A common interest in the problem, plus complementary facilities and data collections, led to collaboration between NOAA's Experimental Meteorology Laboratory and the Space Science and Engineering Center in developing a rainfall estimation technique to help meet this need. During the first year, EML was to provide gage calibrated radar data and expand the echo area rainfall relationship. SSEC was to assemble ATS-3 satellite data, and process radar and satellite data on facilities including the Man-computer Interactive Data Access System (McIDAS, nee WINDCO). This interim report describes SSEC's participation in the first year of the program to develop a method of estimating rainfall from geosynchronous satellite images.

II. Status of the Present Program

Under the first year contract, SSEC proposed to do the following:

1) Digitize, navigate, remap and brightness-normalize (where necessary) about 100 ATS III tape images;
2) Digitize and navigate about 100 of EML's radar images corresponding to the ATS images described above;
3) Secure from NASA about 20 digitized NIMBUS infrared images (if available for the ATS and radar images described above);
4) Operate McIDAS on the ATS, radar, and infrared images to give measurements and correlations of brightness, brightness contour area, echo

area, echo intensity, and infrared contour area;

5) Develop, with EML, tentative relationships between brightness and rainfall; and

6) Evaluate this approach to the problem of estimating rainfall in the tropics, particularly for GATE.

Most of these objectives have been met. Others, not anticipated, have been added; a few remain to be cleared. The method, as it is now configured, is outlined below.

By this method, there are three links in the chain leading from satellite pictures to rainfall estimates. The first is to define the cloud; the second is to relate cloud area to associated echo area; the third is to relate echo area to volumetric rainfall. The last of these links has been forged by EML; graphs exist which relate echo area to rainfall for echoes both growing and shrinking in rain production. (Woodley, Sancho and Miller, 1972; Woodley, Simpson and Miller, 1973). Forging the first and second links is the object of the present program. To define the cloud, we relate maximum cloud brightness to probability of precipitation. The selection of some threshold precipitation probability fixes a threshold cloud brightness level. The cloud area so defined is then directly related to the area of associated echoes, through the whole lifetime of the cloud. This yields a time dependent relation between cloud area and echo area, and the chain is complete.

Data collection and quality

The summer 1972 field program of EML, involving an intercomparison and calibration of two collocated 10-cm radars over a high density raingage network, offered an opportunity to assemble an exceptional basic data set for re-establishment of the cloud brightness-rainfall relation. SSEC made arrangements with the Wallops Island Ground Station for the production of gain controlled, documented daily series of taped images for July and the first three weeks of August. Signal saturation, unfortunately not detected until the end of July, limits to some extent the usefulness of July near-noon pictures; however, examination and use shows the data to be of generally good quality--one of the best sets in the ATS archive. ATS-3 and WSR 57 10-cm radar data for the Experiment period are summarized in Table 1. In addition to satellite and radar coverage, Table 1 indicates by an index combining overlapping coverage and convective activity in radar and satellite images, the usefulness of each day's data for establishing cloud-rainfall relationships. Data days in Table 1 also are randomly divided into analysis and verification classes, the former to be used in establishing a cloud area-echo area relationship, the latter to be used in testing its usefulness in estimating rainfall. Days classified as "good" have been processed first, and within that subset, days of digital coverage before days of analog coverage. On four of the eleven days so far examined, data deficiencies stalled processing: with ATS the problems are bad navigation for 7 August, and poor digitization of analog tapes for 16 August.*

Data processing

Given the newness of the data processing method and system, the substantial initial investment in time, effort and hardware, and the limited quantity of suitable data, it was felt that far more would be gained through increased confidence in the results than would be lost in extra processing time, if, from the very beginning, emphasis was placed not so much on volume of output as on quality and completeness. Although this meant slow processing of the data, analysis of the processed data amply validated this emphasis. Not properly anticipated were additional delays caused by breakdown in the McIDAS system, the demands of other users, and the tediousness and complexity of completely

---

*Unfortunately, no infrared data were available for the summer 1972 period.

TABLE 1

Review of Summer 1972 Basic Data Set and Classification into Analysis and Verification Sets

DATE	DAY	WORKING DAY (yes/no)	DATA 1530-1930Z RADAR (yes/no)	DATA 1530-1930Z ATS (yes/no)	1 HR OR MORE OVER-LAPPING RADAR & ATS 1500-2000Z (yes/no)	MOD-HVY OR HVY-HVY RADAR >10% ATS ACTIVITY (yes/no)	SUBSET (good, poor, nil)	CLASSIFICATION analysis	CLASSIFICATION verification	REMARKS
July	187	yes	yes	yes	yes	yes	good		X	
	188	yes	yes	no	no	yes	nil	X		
7	189	yes	yes	yes	yes	no	poor	X		
	190	no								
	191	no								
10	192	yes	yes	yes	yes	yes	good	X		P
11	193	yes	yes	yes	yes	yes	good	X		
2	194	yes	yes	yes	yes	yes	good		X	
3	195	yes	yes	yes	yes	yes	good	X		P
14	196	yes	yes	yes	yes	yes	good	X		
5	197	no								
6	198	no								
17	199	yes	yes*	yes	yes	yes	good	X		P partial radar cov.
3	200	yes	yes	yes	yes	yes	good	X		P
19	201	yes	yes	yes	yes	yes	good		X	
)*	202	yes	yes	yes	no	yes	poor	X		
l	203	yes	yes	yes	yes	no	poor		X	
22	204	no								
23	205	no								
4	206	yes	yes	yes	yes	yes	good	X		
5	207	yes	yes	yes	no	yes	poor		X	
26	208	yes	yes	yes	yes	no	poor	X		
7	209	yes	yes	yes	yes	no	poor	X		
3	210	yes	yes	yes	yes	no	poor	X		
29	211	no								
30	212	no								
l	213	yes	yes	no	no	no	nil		X	

DATE	DAY	WORKING DAY (yes/no)	DATA 1530-1930Z RADAR (yes/no)	DATA 1530-1930Z ATS (yes/no)	1 HR OR MORE OVER-LAPPING RADAR & ATS 1500-2000Z (yes/no)	MOD-HVY OR HVY-HVY RADAR >10% ATS ACTIVITY (yes/no)	SUBSET (good, poor, nil)	CLASSIFICATION analysis	CLASSIFICATION verification	REMARKS
Aug	214	yes	yes	no			nil	X		
	215	yes	yes	no			nil		X	
3	216	yes	yes	no			nil		X	
4	217	yes	yes	yes	yes	no	poor		X	
	218	no								
6	219	no								
7	220≠	yes	yes	yes	yes	yes	good	X		Bad navigation problems
	221	yes	yes*	yes	yes	yes	good	X		P no radar times
9*	222	yes	yes	yes	yes	yes	good	X		
0	223	yes	yes	yes	yes	no	poor	X		
11	224	yes	yes	yes	yes	no	poor	X		
12	225	no								
3	226	no								
4	227	yes	yes	yes	yes	yes	good		X	P
15	228	yes	yes	yes	yes	yes	good	X		P
16	229®	yes	yes	yes	yes	yes	good	X		Bad can't digitize
17*	230	yes	yes	yes	yes	yes	good	X		P.
8*	231	yes	yes	yes	yes	yes	good		X	

*Found to be incomplete
≠navigation problem
®bad tapes
Pprocessing completed or underway

Ground Rules for Classification: random assignment

Separate total data set into July and August subsets (possible saturation/no saturation)

Separate total data set into good, poor and nil data, subsets, which are defined as

good - at least 1 hour overlapping ATS and radar within 1/2 hrs of local solar noon-1500Z to 2000Z, plus moderate-heavy or heavy-heavy radar activity over land <u>or</u> >10% ATS cloud activity (average for F. Florida) during overlap period

nil - no radar or no satellite data 1530 to 1930Z

poor - all other

Randomization is such that 2/3 to 3/4 of all good and all poor days go into analysis subset.

documenting all clouds and echoes in a multiple picture series. Equipment problems included failure of the analog disk in September, which delayed loading of the first radar and satellite images until December; and intermittent failures in the Raytheon 440 computer system, which delayed digitization and loading of images on the disk.

In spite of these difficulties, processing is complete through frequency distributions of brightness for 950 echoes and 1300 clouds--five days of data. Two additional days, including one for verification, are on the disk, ready for frequency distribution processing. An eighth day awaits radar processing and loading.

Processing steps leading to the determination of maximum cloud brightness and cloud and echo areas are shown schematically in Figure 1. Radar images are converted to digital data by means of a digitizer which scans glossy prints made from the original radar microfilm. Range lines and ground clutter on these prints are painted out, leaving only echoes and selected navigation points. Portions of the digitized image containing navigation points ("landmarks") are loaded on McIDAS for display and line-element location of landmarks. Once landmarks of known latitude and longitude are located in line-element coordinates for the whole picture sequence, the sequence is navigated by means of a program which assigns a latitude and longitude to every point in the line-element coordinate frame. Following navigation, each image is remapped to a cylindrical equidistant projection. The digitized, navigated, remapped images are then loaded in sequence on the McIDAS analog disc (Figure 2a).

Images from ATS-3 undergo a similar processing. If in analog form, they are first digitized. The digital data are run through a quality control program which checks for digitizing quality, signal levels, line and element

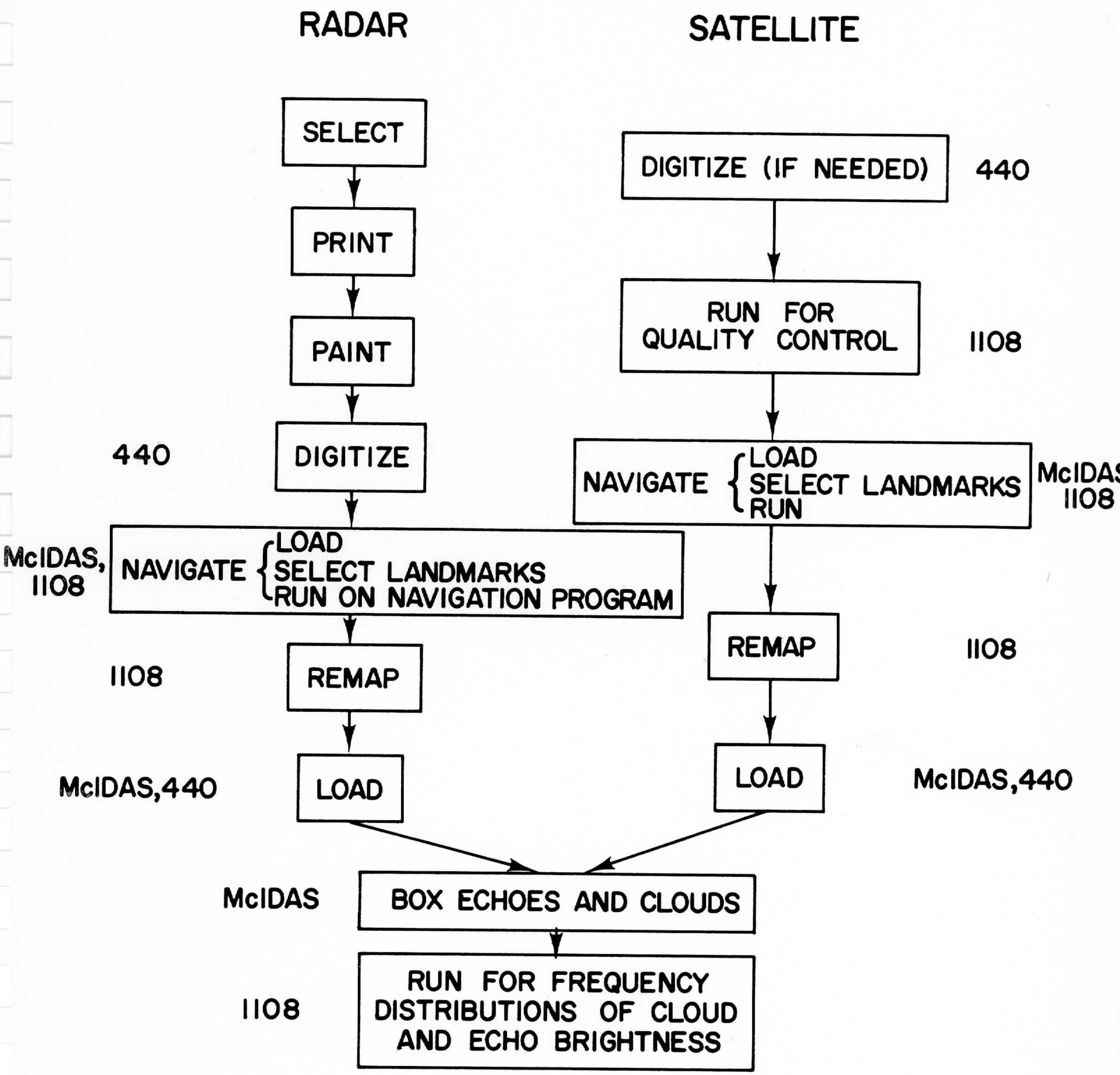

Figure 1. Steps involved in radar and satellite data processing. Labels adjacent to boxes indicate systems used for processing; 1108~ Univac computer, 440~ Raytheon computer. See text for further explanation.

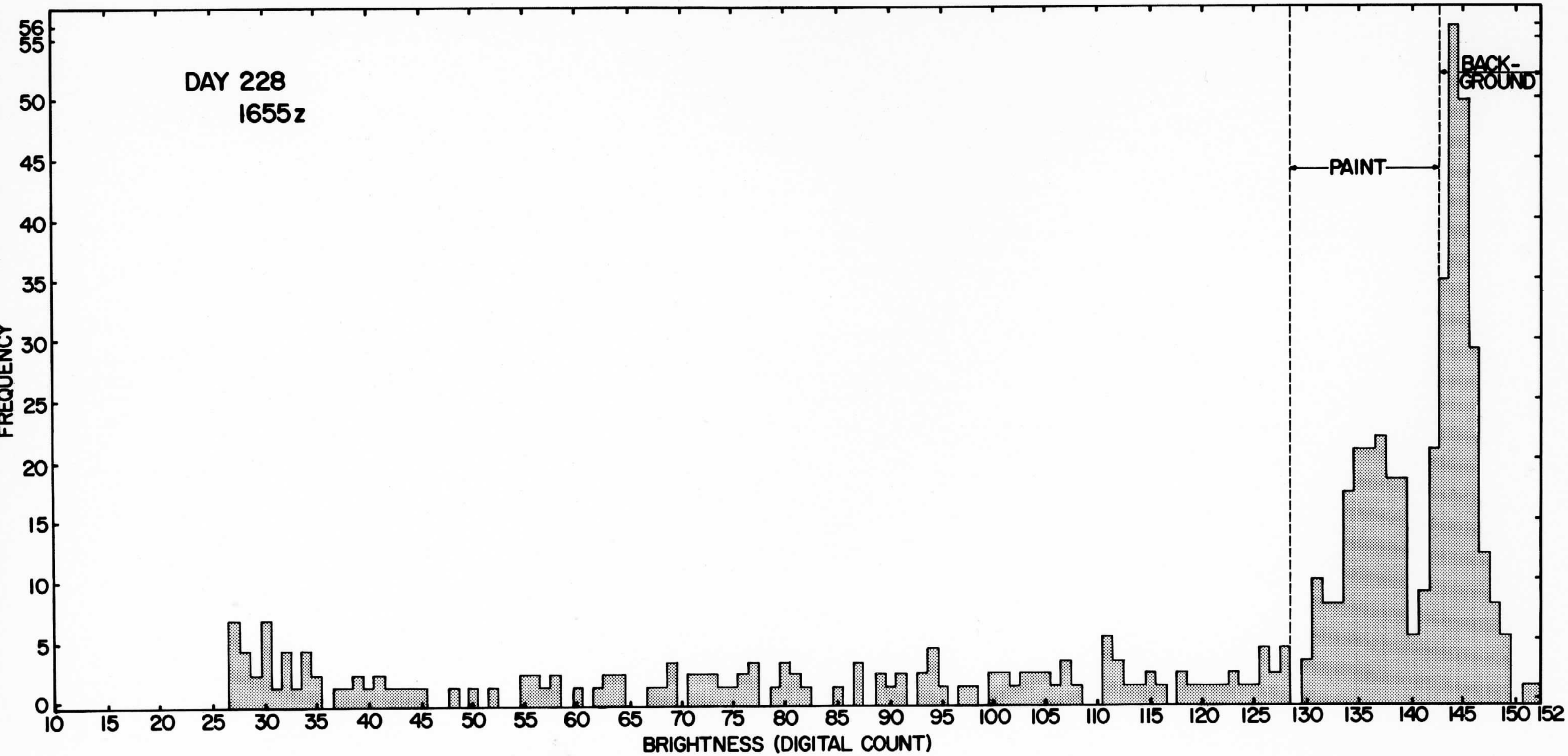

Figure 5. Frequency distribution of brightness for a single large echo. Radar scope background and painted area distributions are indicated. Although this was a second level echo, there is no clear distinction between the distributions for the first and second intensity levels.

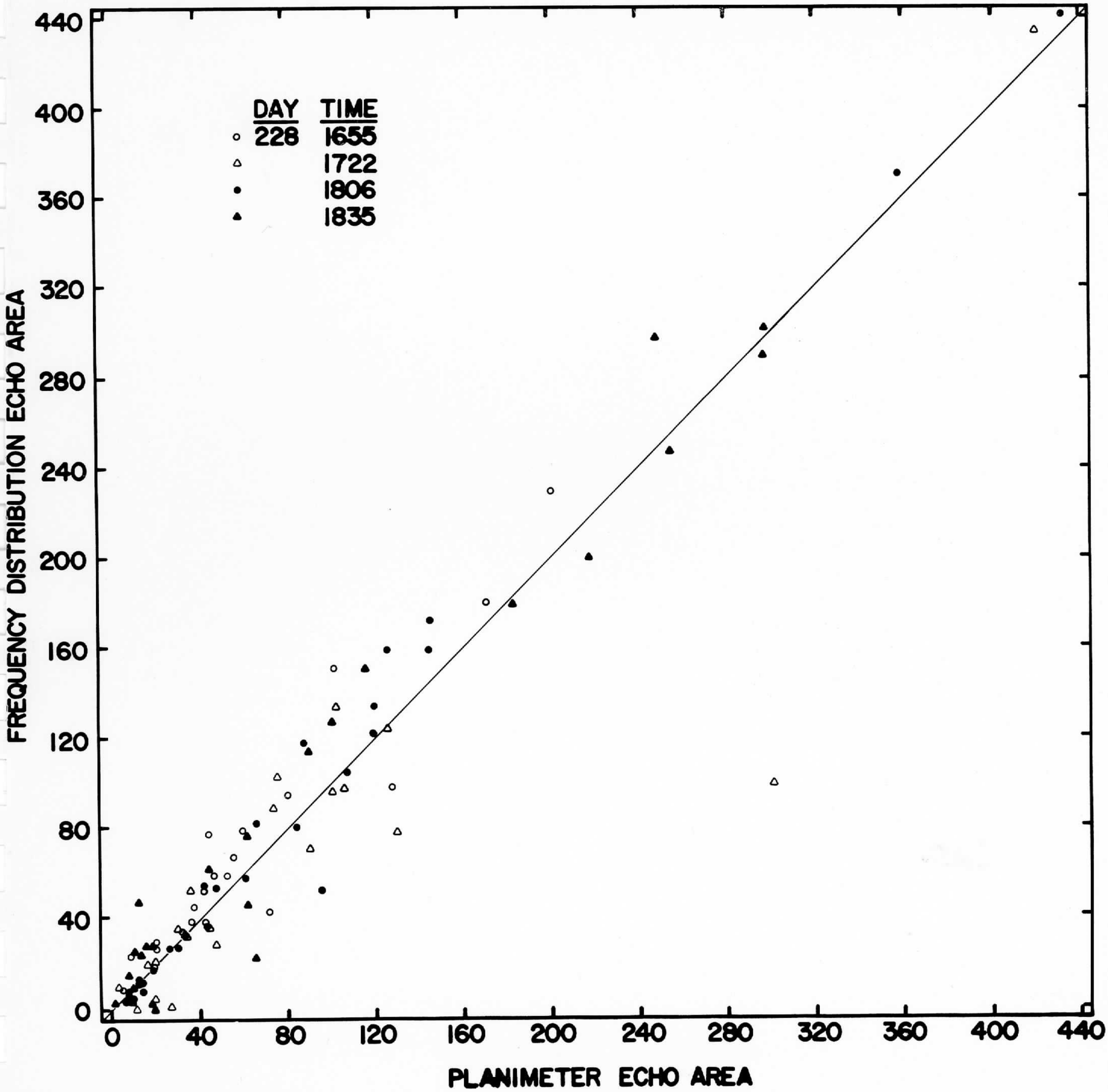

Figure 6. Comparison of day 228 echo area estimated from brightness frequency distributions and planimetered from much enlarged radar pictures. Echo area is defined by the first intensity level.

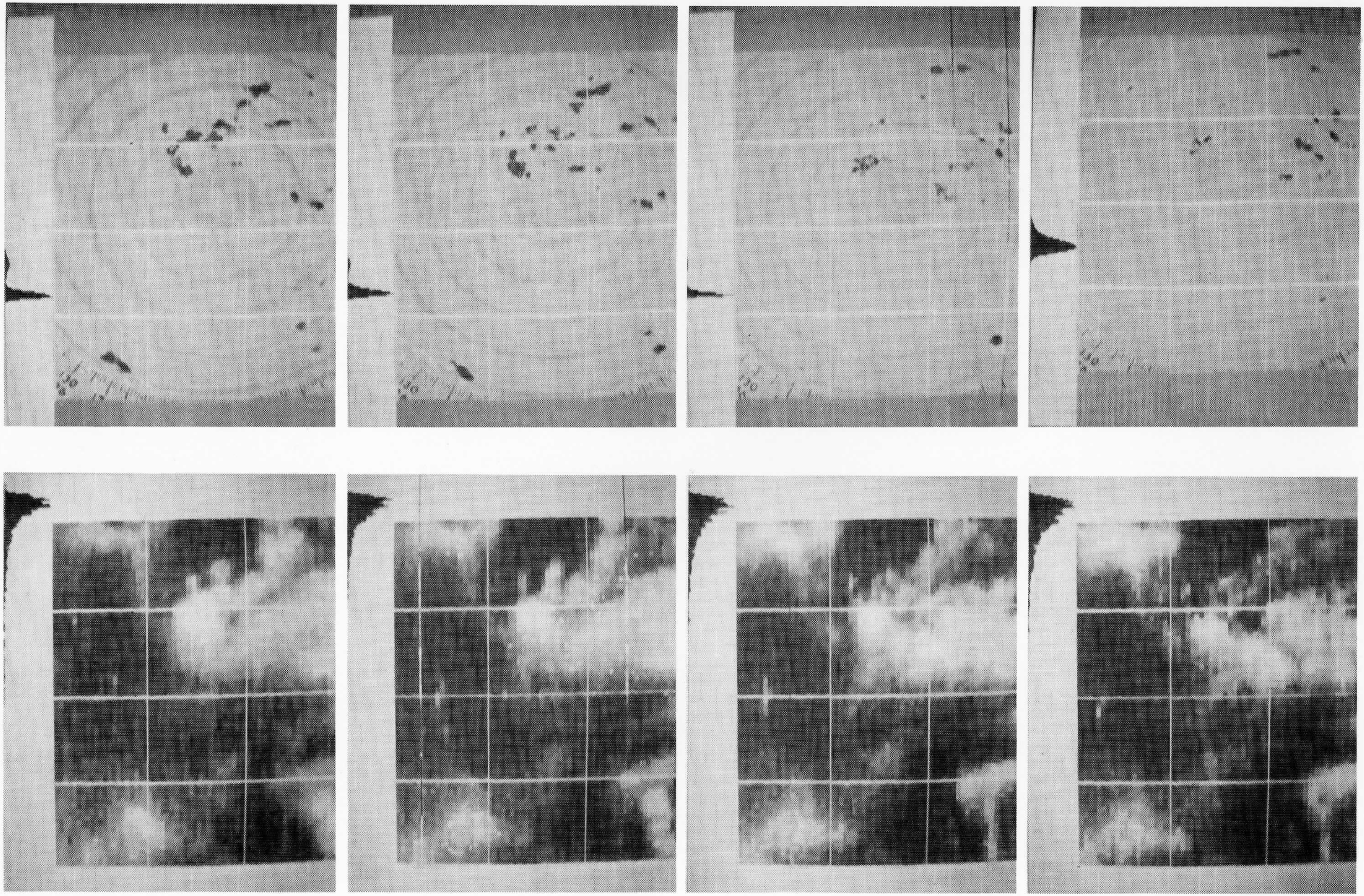

Figure 2. Remapped radar images (left) and ATS-3 images (right) for day 228 (15 August) 1972. A frequency distribution of brightness appears below each image. The separation between grid lines is one degree. ATS-3 images are auto-enhanced. Even in this short sequence, the importance of stage of development in explaining cloud-echo association is apparent; for example, the large cloud mass in the lower left (SW) corner of all ATS images shows an echo only in the first picture pair; however, its steady decline in overall brightness and increasing diffuseness suggests an old, inactive and dissipating thunderstorm complex. A rainfall estimate for this system would miss badly unless stage of development were considered.

level changes, and extensive saturation. Navigation is accomplished through the same load, landmark selection, and run steps used for radar: however, because of the greater number of variables in satellite navigation and the poorer location of landmarks, satellite navigation invariably is less accurate than radar navigation. Once a satisfactory satellite navigation is achieved, the area surrounding south Florida is remapped for each image to a cylindrical equidistant projection identical in scale to the scale of the remapped radar images. ATS-3 images are loaded in normal (unenhanced) and auto-enhanced modes (Figure 2b). In an auto-enhanced picture, the actual brightness range is digitally extended over the total brightness range of the display system (Figure 3). Auto-enhancement allows surer determination of cloud boundaries and identification of small clouds on days of suppressed convection. Unenhanced images are paired in sequence with their radar counterparts; the auto-enhanced images are loaded separately in sequence.

Following completion of the steps outlined above, meteorologists label clouds and echoes and determine coordinates of a box around each cloud and echo for computer calculation of the frequency distributions of brightness that are used to generate cloud and echo areas. (Details of this procedure are presented in the Appendix.) The loop projection capability of McIDAS becomes indispensible in this stage of the processing, for without the time lapse dimension it provides, following the evolutionary development of clouds would be almost impossible.

The association of clouds and echoes is accomplished in two steps: (1) navigation as described of each radar and satellite image achieves collocation generally to within 10 to 20 n mi, and (2) manual shifting of an echo tracing on the basis of small echo and small cloud pattern matching achieves collocation of 1 to 5 n mi, the larger discrepancies resulting mainly from residual distortion

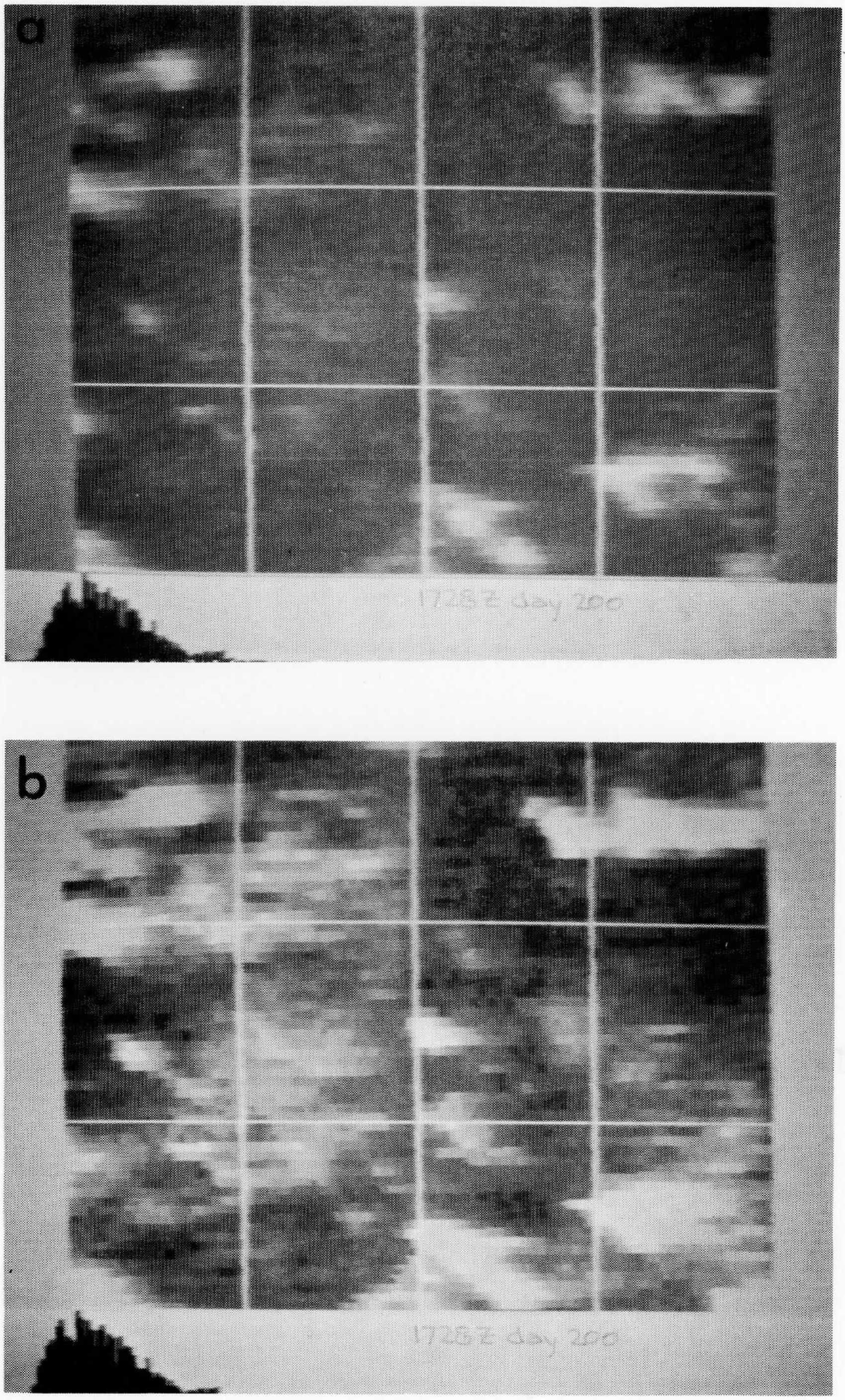

Figure 3a. ATS-3 image displayed on the WINDCO monitor; no enhancement applied.

b. The same ATS-3 image, autoenhanced. The frequency distribution of brightness represents the original unenhanced data.

in the remapped images. In almost all cases the subsequent association of clouds and echoes is unequivocal. An example of this operation is given in Figure 4.

Data analysis

The processing which satellite and radar images undergo results in two primary products: frequency distributions of brightness for boxes enclosing each cloud and echo, and a number identification for each cloud and echo. The identification associates clouds with their corresponding echo or echoes and allows the analyst to follow any cloud or echo through its entire evolution. It also indicates much of the life history of the cloud/echo, including order of appearance of clouds and echoes, age of clouds and echoes, and mergers and divisions. Frequency distributions of brightness allow determination of two important statistics: maximum cloud brightnesses, and areas of clouds and echoes at specified brightness levels.

Frequency distributions of brightness are produced from the remapped digital tapes. Echo areas are calculated from these distributions by selecting, on the basis of frequency distributions of background and painted areas, a brightness cut-off level (Figure 5). All samples below the cut-off level are considered to represent echo area. Tests of this method suggest that for determination of total echo area, it is as good and possibly better than manual methods in routine use (Figure 6). Frequency distribution estimates of echo area at the second intensity level are less successful, apparently because of a reduced contrast between intensity level densities. Strong echoes having a third or higher level* are handled in two steps--an outer box for the whole echo and an inner box for the third level core, or more often are simply measured for area by manual methods.

---

*1972 radar images were contoured in three steps of grey, the third level having the same density as the scope background.

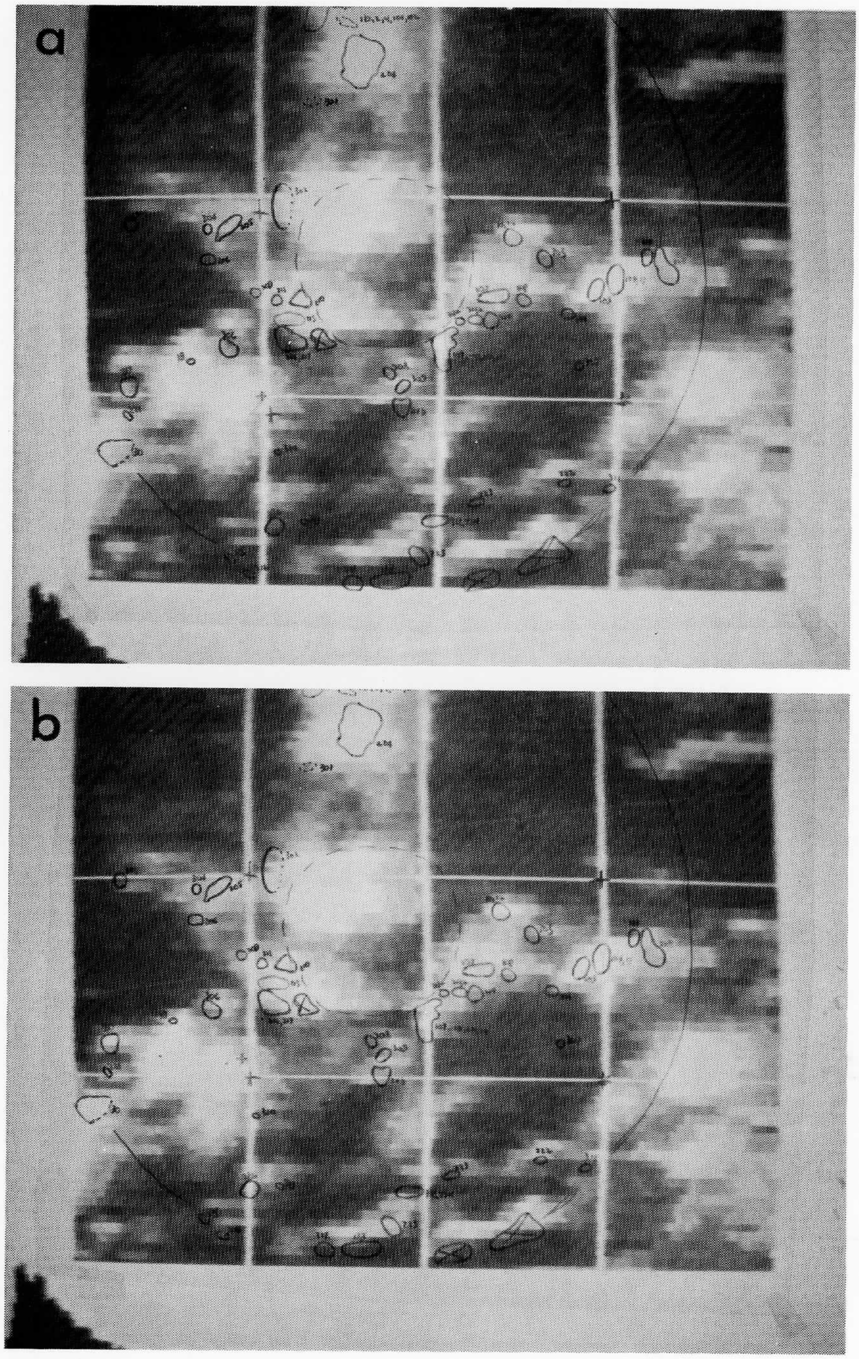

Figure 4a. Echo tracing for 1713z, day 230 (17 August), superpositioned by individual, independent radar and satellite navigations.

b. Cloud and echo fields superpositioned by original navigation plus pattern matching small echos and small clouds.

Cloud area depends upon the brightness contour used to define the cloud. Selection of a best brightness level or levels is accomplished by developing a relationship between maximum cloud brightness and precipitation probability. Treating each day individually, clouds first are stratified by maximum digital count (brightness) in intervals of ten digital counts. The ratio number-of-clouds-with-echoes divided by number-of-clouds is computed for each interval, then plotted against maximum digital count (Figure 7, 8a,b). "With echoes" is defined in two ways--one level only (minimum detectable signal) echoes, and two or higher level echoes--resulting in two points for each digital count interval. As echoes are indicators of precipitation, the points on such a graph represent probability of precipitation as a function of maximum cloud brightness.

On the basis of five such curves, four brightness levels (40, 50, 60 and 80 digital counts) have been selected for defining clouds. In this early stage of analysis the use of several levels allows some flexibility in establishing cloud area-echo relationships; it also obviates temporarily the need to standardize July and August data to a common gain level. Cloud areas, echo areas, maximum cloud brightness, and maximum echo intensity level are tabulated for each cloud through the whole of its life. From such tables, plots are made showing, for individual clouds, time changes of areas and maximum brightness (Figures 9 a, b, c, d). The combination of individual cloud-echo plots is accomplished by normalizing the time scale on the basis of time of occurrence of maximum echo area (Figure 10). Graphs such as these show not only cloud and echo area magnitudes, but time changes, phase relations, and differences from cloud to cloud.

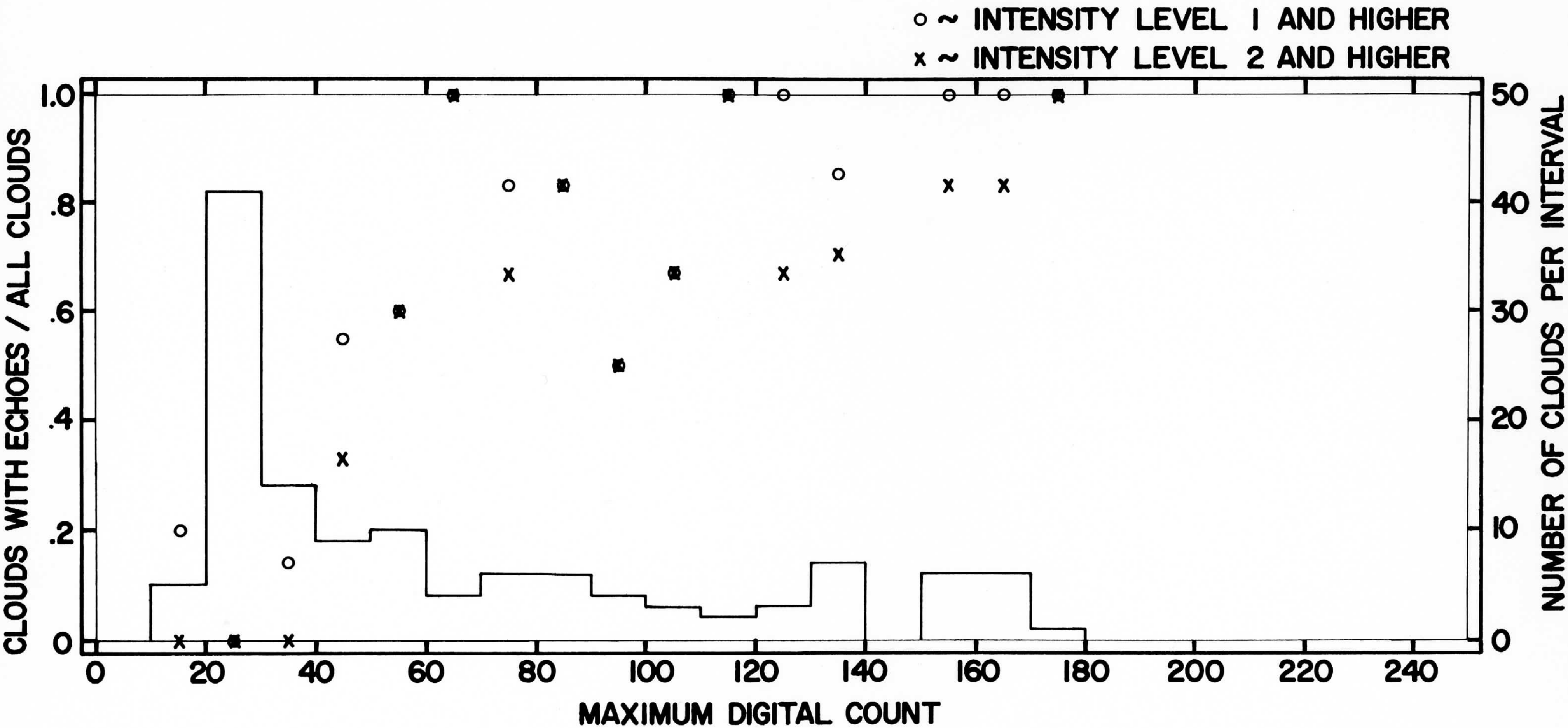

Figure 7. The ratio of the number of clouds with echos divided by the number of all clouds is plotted against maximum cloud brightness (digital count) for intervals of ten digital counts. Data is for day 228. Circles represent echo-cloud ratios for all echos regardless of intensity; crosses represent echo-cloud ratios for all echos except those of level one (minimum detectable signal-MDS) intensity. The number of clouds is shown for each interval by the bar graph. For example, five clouds had maximum brightness between 10 and 19 digital counts. One of these clouds was associated with a level one echo, none with echoes of higher intensity.

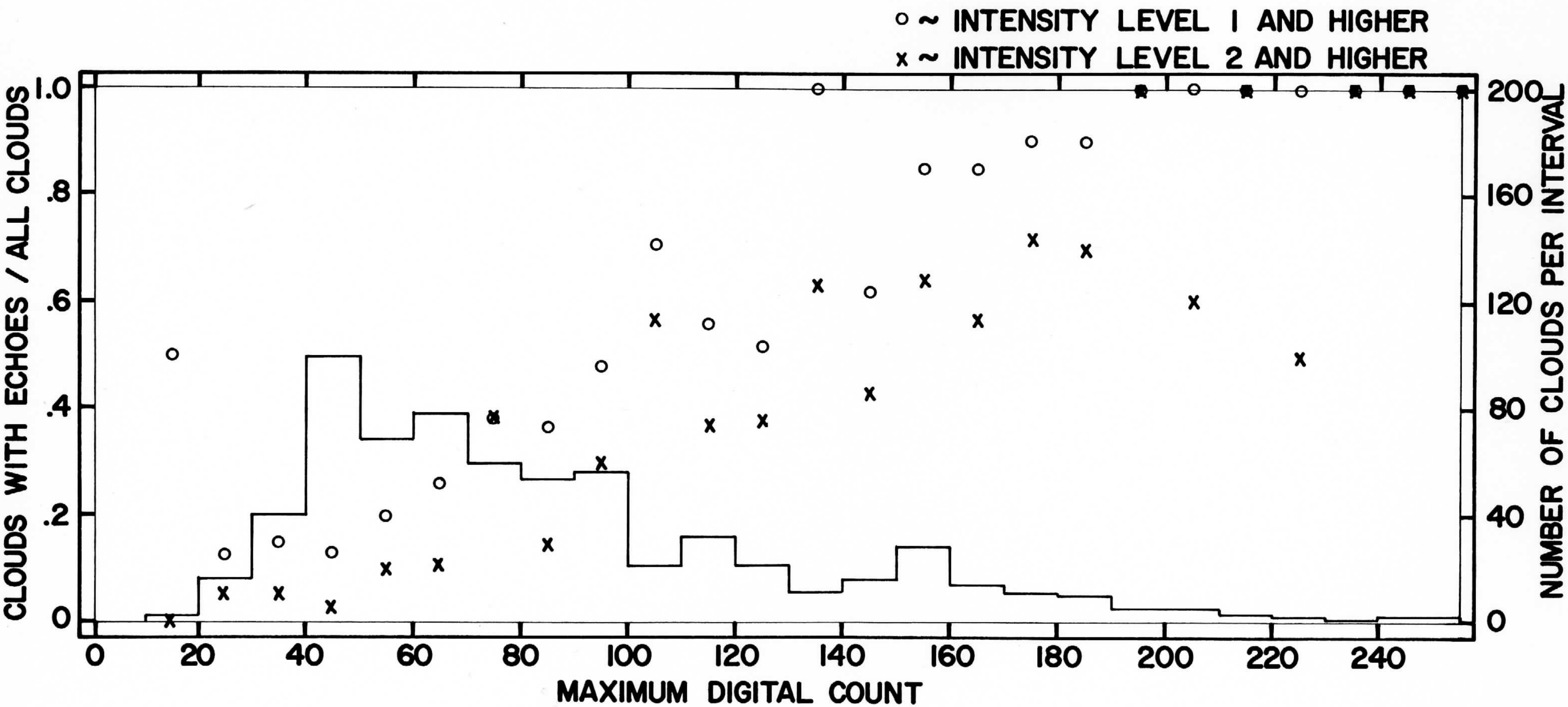

Figure 8a. As for Figure 7, except days 220, 228, and 230 together.

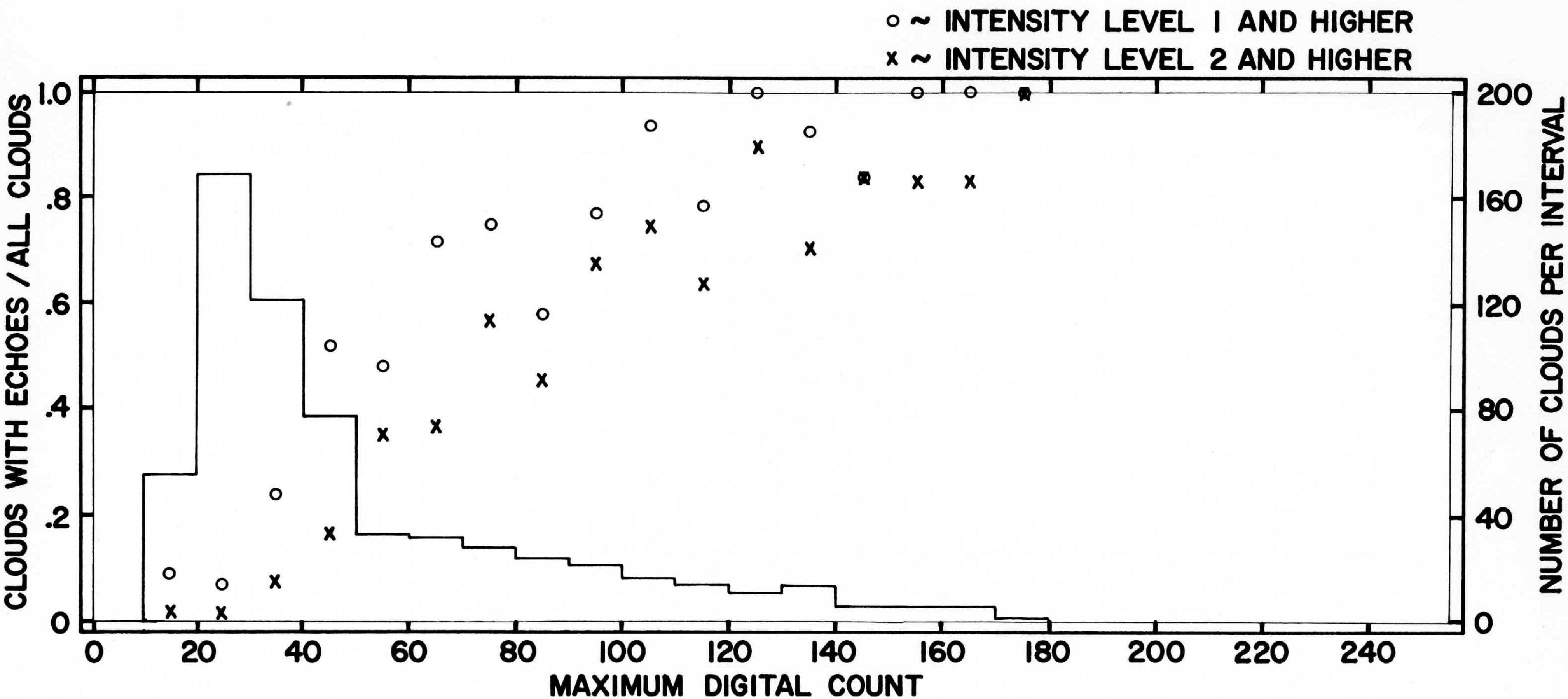

Figure 8b. As for Figure 7, except days 192 and 200 together. Note the decreased slope of the curve from Figures 8a to 8b, reflecting in part a reduction of the ground station gain from July to August.

Figure 9. Cloud area, echo area, and maximum digital count (cloud brightness) are plotted as functions of time for individual clouds. Note that in some cases cloud and echo areas have been plotted on different scales. The brightness level used to define cloud area is indicated at the left end of the cloud area curve. Echo area defined by the first intensity level (minimum detectable signal) is marked 1; area defined by the second intensity level is marked 2. Maximum echo intensity level is given by a number next to data points for echo area. Areas are in units of (0.01 degree latitude)^2.

a. Day 192 (10 July).

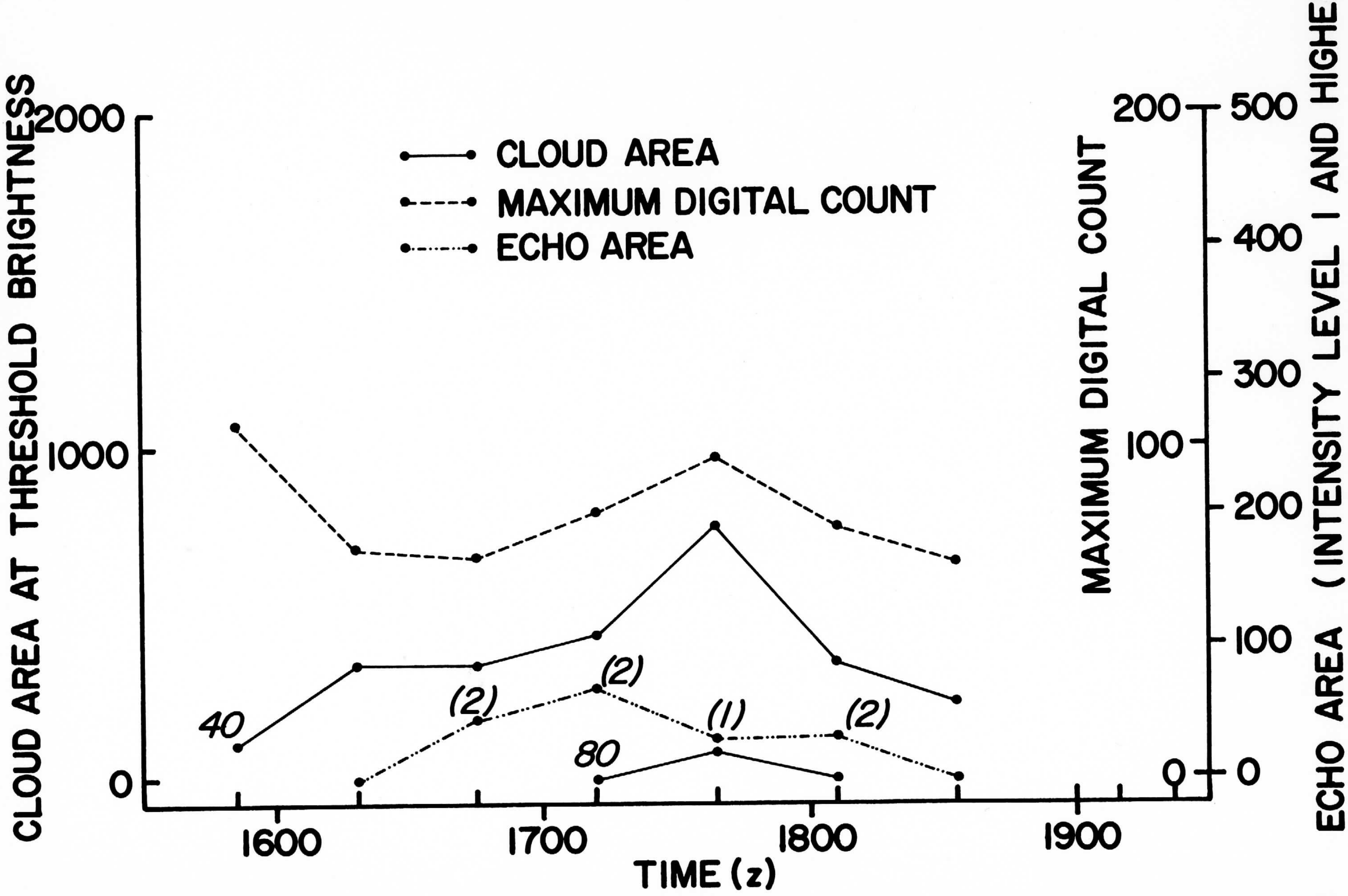

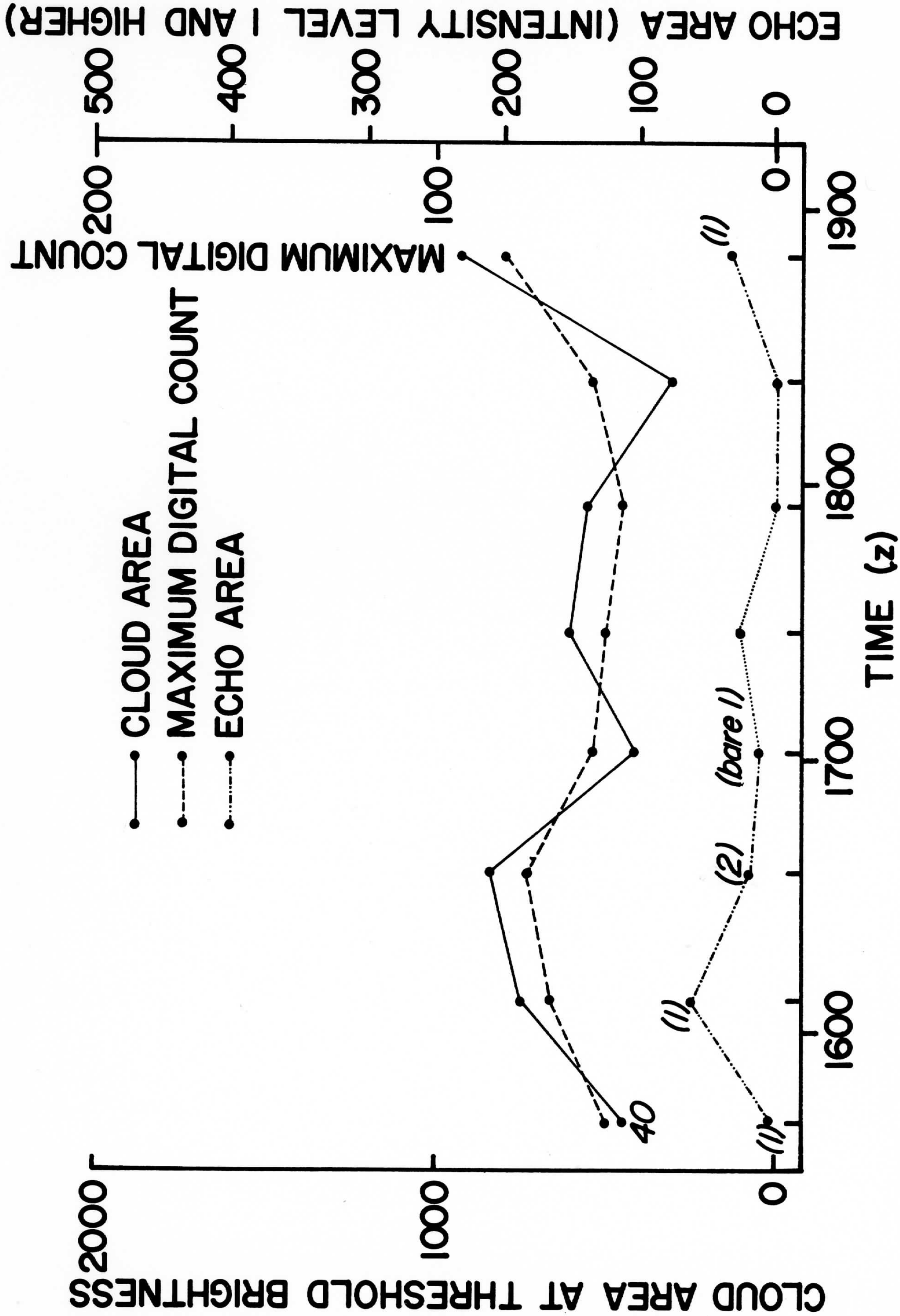

Figure 9b. Day 200 (18 July).

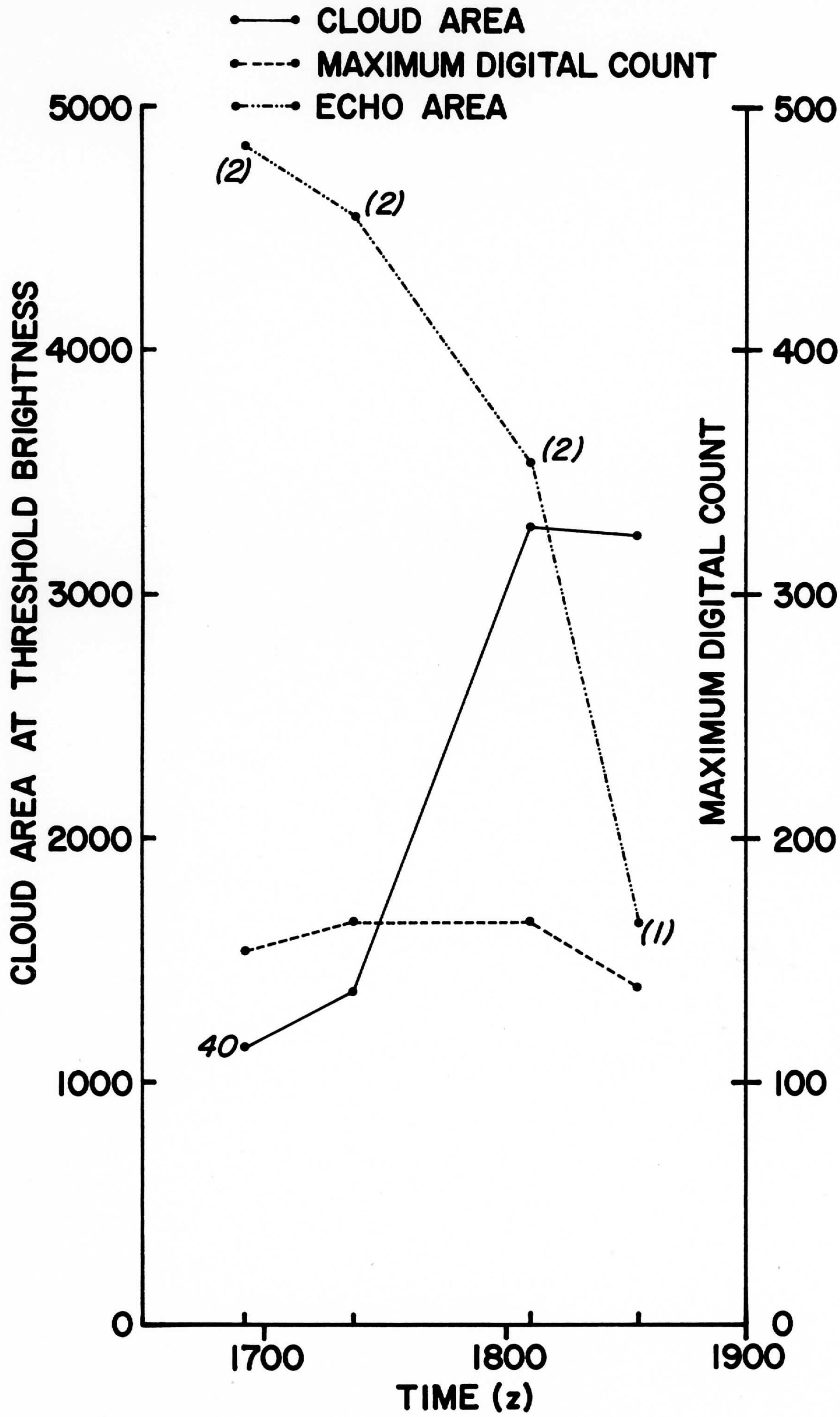

Figure 9c. Day 228 (15 August).

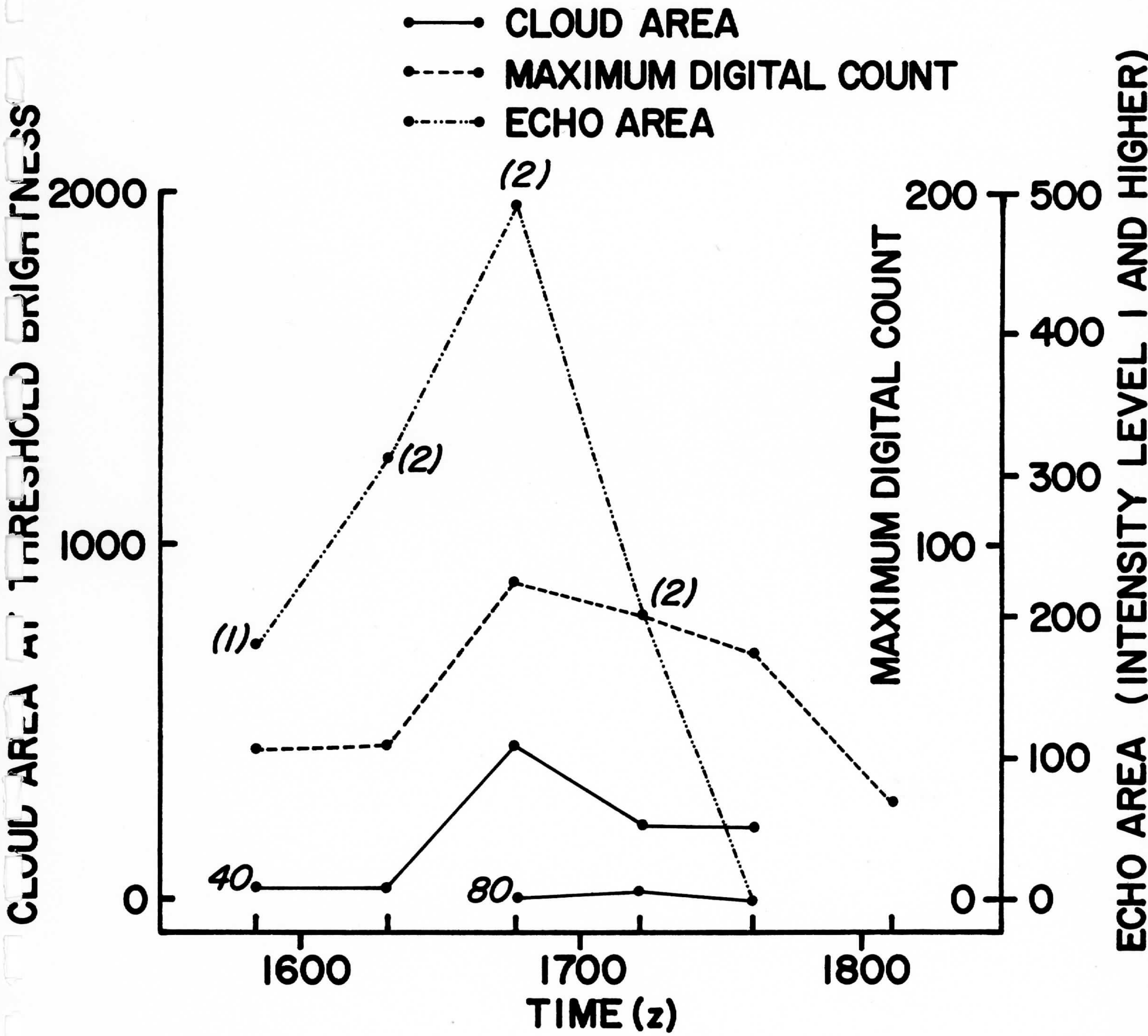

Figure 9d. Day 230 (17 August).

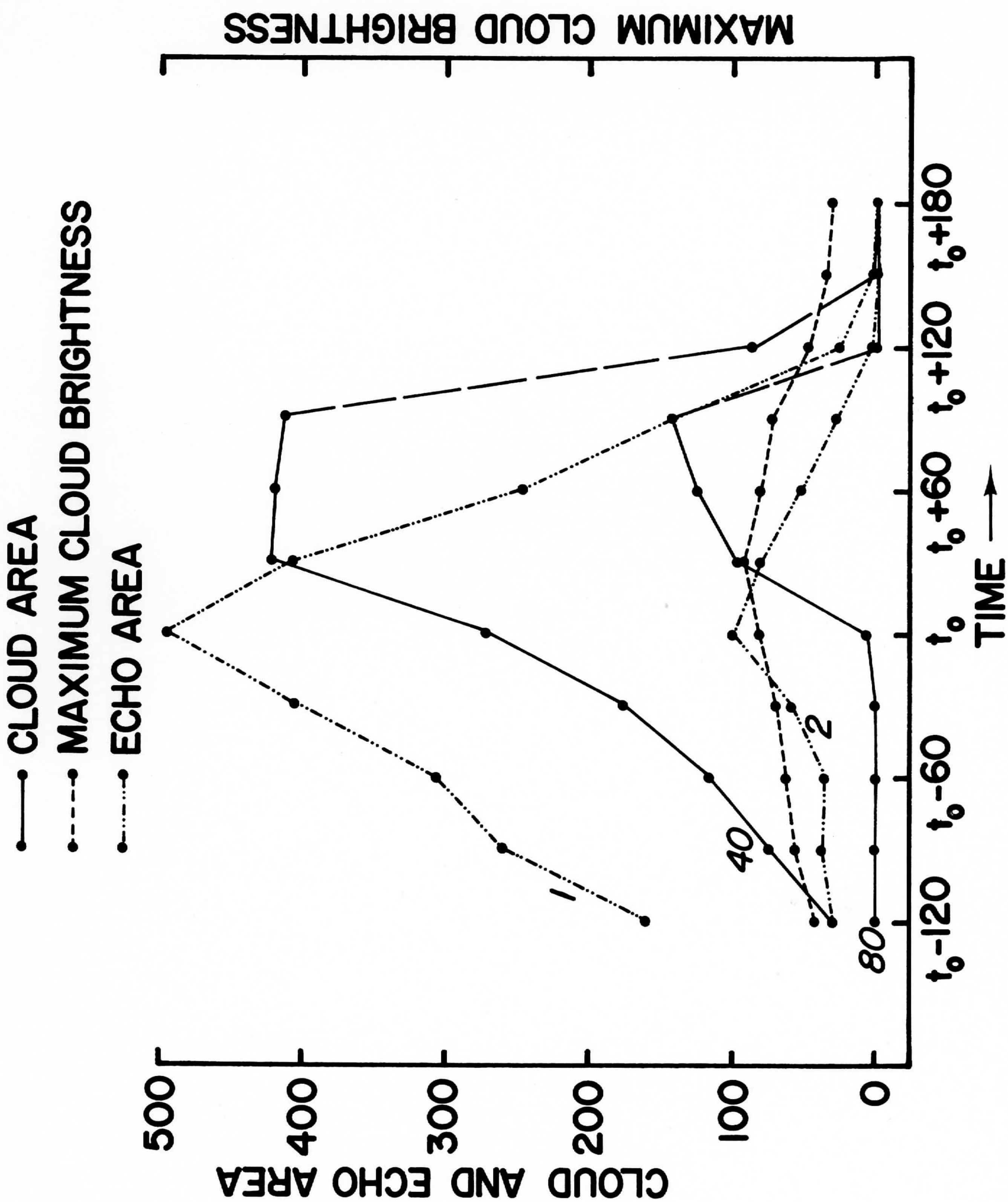

Figure 10. Time changes of maximum digital count and cloud and echo area, composited for three of the best behaved and most completely surveyed clouds on days 228 and 230. Maximum values in the curves of echo area at the first intensity level served as reference points. The total interval is five hours. Numbers on the echo and cloud curves indicate echo intensity level and digital count for area determination.

III. Results to Date

Although analysis of the data continues, a sufficient sample has been examined to warrant these conclusions.

1) There is a strong relationship between clouds and echoes (Figure 4, Figure 11a, b, c, d). This is apparent in even a casual superposition of cloud and echo fields on McIDAS. Such discrepancies as do exist are accountable through consideration of stage of development, and to a lesser extent, resolution limitations of the satellite and residual distortion in the remapped images.

2) Convective clouds over and adjacent to South Florida show a remarkable range of regimes--i.e., day to day differences in frequency, size and behavior--and, more often than not, a mind-taxing complexity. These differences are apparent in comparisons of daily pictures (Figures 2 and 9a, b, c, d). Day 192 (10 July) was dominated by a cluster-type system producing extensive persistent but light rainfall. Numerous echoes on day 200 (18 July) tended to clump. Clouds appeared as small clusters and squall-like systems. Day 222 (9 August) clouds and echoes were small, scattered, and short lived. Clouds and echoes were concentrated over South Florida on day 228 (15 August), but again were widely dispersed on day 230 (17 August) when clouds and echoes tended to appear in lines and bands.

3) On a linear brightness scale of zero to 1 (space to the brightest cumulonimbi), a maximum cloud brightness of 0.3 implies roughly 50% probability an echo is present (Figure 8a, b). At a brightness level of 0.1 this probability is ~10%, at 0.5 it is ~75%.

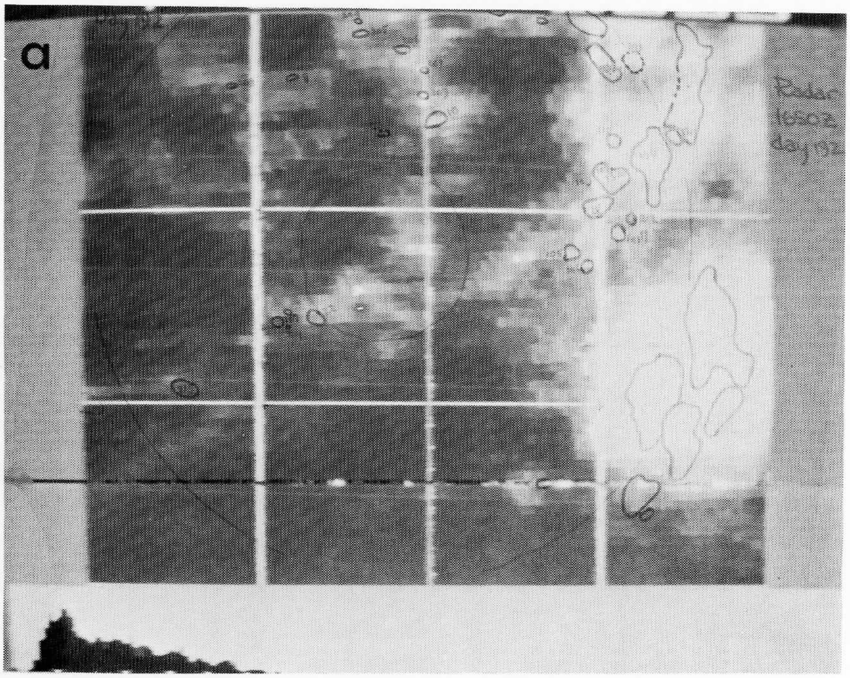

Figure 11. Radar echo tracings superimposed over simultaneous ATS cloud fields. Local noon at Miami occurs at 1720z.

a. 1650/1645z day 192.

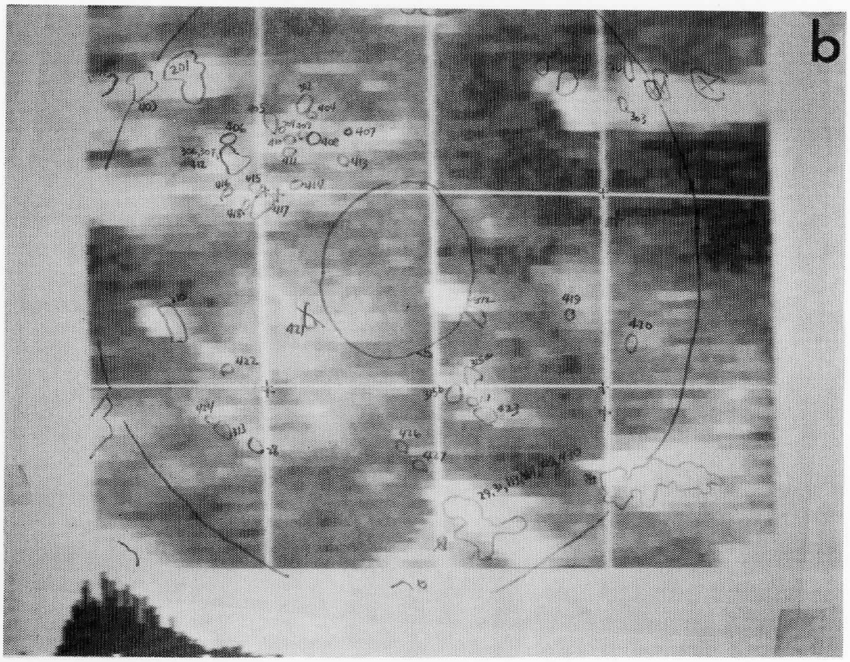

Figure 11b. 1737/1728z day 200.

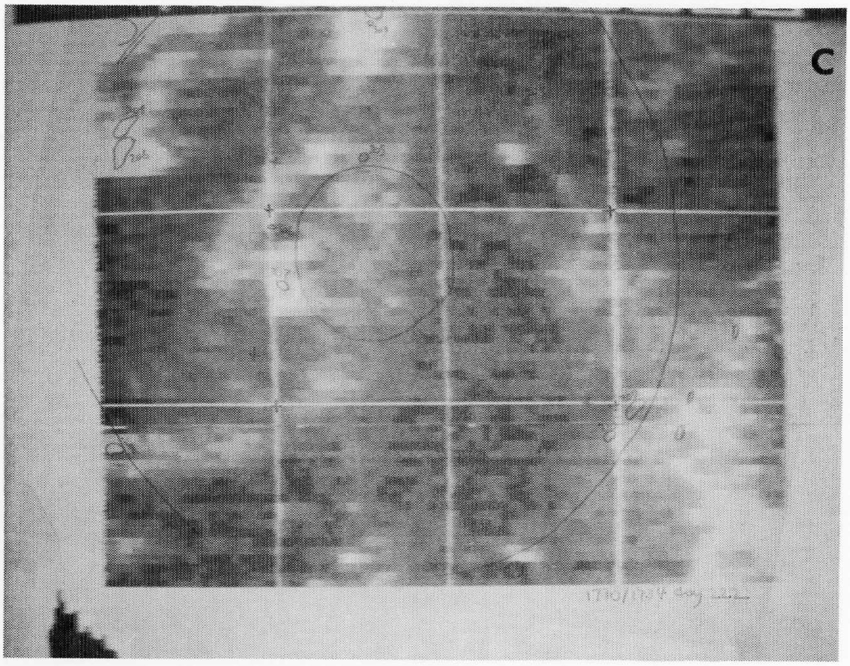

Figure 11c. 1734/1730z day 222.

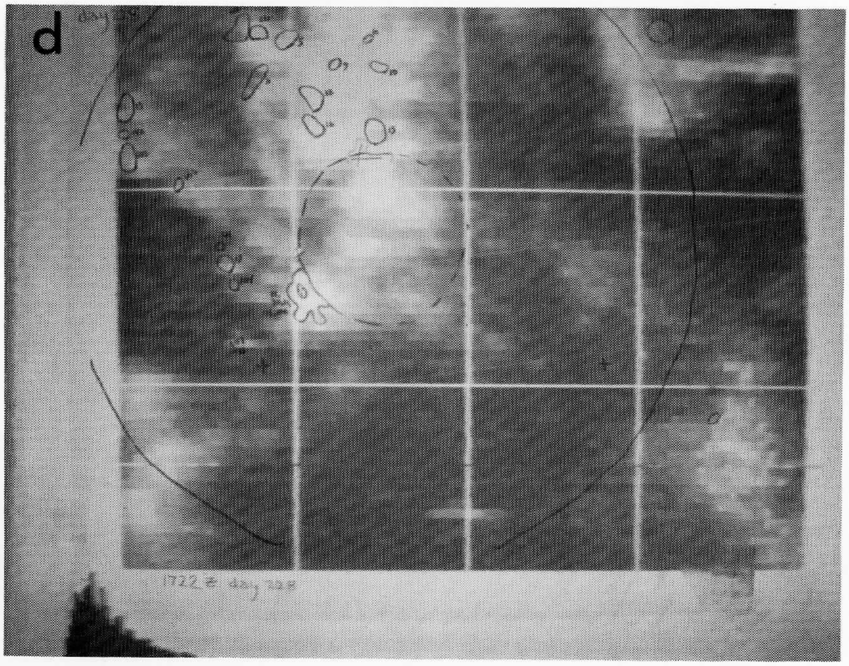

Figure 11d. 1722/1718z day 228.

4) Plots of cloud and echo area change for two days show that maximum cloud area occurs later as threshold brightness is increased; echo and cloud area changes are slightly out of phase, with echo area leading by 1/2 to 1 hour; and maximum cloud brightness occurs after maximum echo area (Figure 9 a, b, c, d and Figure 10).

5) Unquestionably, cloud brightness has value as an indicator of precipitation. Inclusion of stage of development promises substantial improvement in the accuracy of precipitation estimates made from satellite images. Given a reasonably high sampling frequency and adequate controls on the satellite signal, the method as proposed can provide meteorologically useful estimates of rainfall for GATE.

Some of these results have already been conveyed to the meteorological community: in a conference, "Rainfall Estimation from Satellite Images," sponsored by SSEC on 12-13 December 1972; and in a paper, "Possibilities of Rainfall Estimates Using Satellite Observations," presented with William L. Woodley and Verner E. Suomi at the American Meteorological Society's 53rd Annual Meeting in January 1973. This contract also has supported one author (Martin; co-author is Wolfgang D. Scherer) of an article, "Review of Satellite Rainfall Estimation Methods," to appear under "GARP Topics" in the July 1973 issue of the AMS Bulletin.

REFERENCES

Woodley, William L., Joanne Simpson, and Alan Miller, 1973: GATE Research at the Experimental Meteorology Laboratory, 31 pp.

Woodley, William L., B. Sancho, and A. H. Miller, 1972: Rainfall Estimation from Satellite Cloud Photographs, NOAA Technical Memorandum, ERL OD-11, 43 pp.

Space Science and Engineering Center, 1972: McIDAS: an Interim Report on the Development of the Man-Computer Interactive Data Access System, University of Wisconsin, Madison.

APPENDIX

Radar - ATS Image Processing on McIDAS I

I. First cloud echo image pair

1. Trace radar echo pattern
2. Number radar echoes beginning with 1, place crosses at grid intersections, take boxes enclosing echoes.
3. Superimpose for best fit of small clouds and small echoes the echo tracing over the corresponding cloud pattern
4. Mark grid intersections
5. Remove echo tracing, trace cloud field on new sheet of acetate. Use 2 contours, black for cloud/clear boundary, some other color for individual clouds. Include as much of the cloud as is practical.
6. Remove cloud tracing, superimpose echo tracing on cloud image, shift as needed to get best fit between small clouds and small echoes. Place cloud tracing over echo tracing.
7. Number clouds according to associated echoes. Clouds with no echoes are numbered from 51. Take boxes enclosing clouds.

II. Second cloud-echo image pair

8. Lay new sheet of acetate over next picture in the radar sequence. Trace radar echo pattern.
9. Remove echo tracing. Lay preceding echo tracing over echo pattern (using grid marks as a guide for placement). Superimpose new tracing over old. Number carryover echoes on new tracing according to their to the echo tracing. Number new echoes from 101. Place crosses at grid intersections.

10. Take boxes enclosing echoes.

11. Change TV frames to display corresponding cloud picture. Remove echo tracing. Place clean acetate over cloud field, trace as in step 5.

12. Remove cloud tracing. Superimpose preceding cloud tracing on cloud field, matching grid intersections. Superimpose new tracing over old, matching grid intersections. Number clouds in new tracing according to associated clouds from previous tracing.

13. Remove new and old cloud tracings. Superimpose new echo tracing according to best fit of small clouds and small echoes (or simply by cloud image grid intersection crosses). Superimpose new cloud tracing, add numbers of new echoes. Remove echo tracing, number new clouds without echoes beginning with 151.

14. Take boxes enclosing clouds.

III. Third echo-cloud image pair

15. Repeat steps 8-14 for next and succeeding image pairs.